Journal of Solid State Electrochemistry (2020) 24:1921–1926
https://doi.org/10.1007/s10008-020-04557-7

ORIGINAL PAPER

Tuning oscillatory time-series evolution by Pt(111)-OH_{ad} stabilization

Kaline N. da Silva [1] · Elton Sitta [1]

Received: 29 January 2020 / Revised: 13 March 2020 / Accepted: 15 March 2020 / Published online: 26 March 2020

Abstract

Controlling the Pt(111)-OH_{ad} stability by means of noncovalent interactions with hydrated cations, it was possible to modify natural changes in the galvanostatic time-series collected during ethylene glycol electro-oxidation reaction. These modifications, also known as *drift*, include maximum potential in each oscillation cycle, oscillation patterns, and frequency changes. The phenomenon was investigated in a temperature range from 5 to 20 °C and allows us to infer about the sensitiveness of time-series in the presence of distinct alkaline cations. The stable OH_{ad} layer in the presence of Li^+ induces lower *drift* in the time-series, resulting in a longer time-series with oscillatory behavior. On the other hand, once the OH_{ad} layer is less stable in the Na^+ electrolyte, the formation of surface oxides from Pt-OH happens at lower potential than in the LiOH solution, resulting in fast changes of both the maximum potential and oscillation frequency and short time-series, i.e., the *drift* becoming higher. Finally, the conversion of Pt-OH onto Pt oxides is still easier in KOH solutions, producing short time-series and does not allow the oscillatory behavior.

Keywords Drift in time-series · Ethylene glycol electro-oxidation · Oscillations · Cation effect · Pt(111)

Introduction

In recent decades, instabilities in electrochemical systems have been studied to understand fuel cell reactions like the hydrogen peroxide electro-reduction[1–3], hydrogen [4], formic acid [5], formaldehyde [6], methanol [7–11], ethanol [12, 13], ethylene glycol [14–16], and glycerol electro-oxidation [17, 18]. Focusing on the electro-oxidation of small organic molecules, oscillations in all the above cited systems can be classified as *N-shaped Negative Differential Resistance* with *N* partially *Hidden* (HN-NDR) [19, 20] and they share features like oscillations under both potential and current controls and changes in oscillation dynamics over time, even under fixed (external) conditions. These changes, called *drift*, can modify the oscillation period, amplitude, and shape or even to extinguish the oscillatory behavior [21].

Electronic supplementary material The online version of this article (https://doi.org/10.1007/s10008-020-04557-7) contains supplementary material, which is available to authorized users.

✉ Elton Sitta
esitta@ufscar.br

[1] Chemistry Department, Federal University of Sao Carlos, Rod. Washington Luis, km 235, Sao Carlos 13565-905, Brazil

Prof. Varela and his group have pointed out that the *drift* is due to the existence of at least two coupled processes, one being fast, responsible for the oscillations, and the other, slower, whose evolution modifies the time-series [6, 22–24]. Irreversible oxide formation, caused by the place exchange between surface O_{ad} and Pt atoms, is frequently associated with the slow process in the oscillations potential window. However, on polycrystalline Pt surfaces, Pt(poly), the species present on the (hydro)oxide onset region are still not fully understood. While early systematic studies from the 1970s [25] suggested that PtO formation is PtOH-mediated in a 1 + 1 electron transfer pathway, more recent works claim that PtO can be directly produced [26] or PtO and PtOH are parallel processes at the same potential [27], probably in distinct surface orientation domains [28]. Regardless of the nature of these species, irreversible processes are observed when the amount of oxygen on the surface is lower than one monolayer (ML) in Pt(poly) [25].

Herein, we explore electrochemical oscillations employing Pt(111) as catalyst that, contrary to all other Pt orientations, can split the three important processes between Pt and H_2O, namely adsorbed hydrogen formation/reduction (Pt-H), OH adsorption/desorption (Pt-OH), and oxide formation/reduction (PtO). Thus, this surface becomes unique to analyze the effect of PtOH and oxides during oscillations in

electrochemical systems. Moreover, due to noncovalent interactions between cations and adsorbed species (OH_{ad} and O_{ad}), the interplay of PtOH and PtO can be modulated in alkaline media changing the electrolyte cation [29]. Finally, the ethylene glycol electro-oxidation (EGEO) reaction in alkaline media was chosen due to its several pattern oscillations with high frequency described in early publications [14–16].

Experimental

The working electrode (WE) was prepared by Clavilier method as described in ref. [30] and the area estimated at 0.045 cm^2 with roughness factor close to one. Before each experiment, the WE surface was flame annealed in a butane/air flame, cooled in reductive Ar:H_2 (3:1) atmosphere and transferred to the electrochemical cell with a drop of ultra-pure water saturated with both Ar and H_2. A high area Pt wire was used as counter electrode and all the potentials were measured and displayed based on the reversible hydrogen electrode (RHE) prepared with the same supporting electrolyte solution [31]. 0.1 M of MOH (M = K, Na, or Li) solutions were prepared dissolving ultra-pure hydroxides (Sigma-Aldrich 99.95%, metal grade) in 18.2 MΩ cm water (Milli-Q system). Ethylene glycol (Sigma-Aldrich 99.8%) was directly added in the electrolyte yielding 0.05 M. An Autolab PGSTAT 128 N equipped with Scan 250 modulus was used as potentiostat/galvanostat and the temperature was controlled with a Solab SL 152 thermostatic bath. Before the experiments, the solution was purged with Argon 5.0 N, and during the data collection, this gas was kept in the cell headspace. The WE surface quality was checked by cyclic voltammetry from 0.05 to 1.0 V (vs RHE) at 0.05 V s^{-1}, and before the current-controlled experiments (galvanodynamic with step of 1.5 μA and rate 44.4 μA s^{-1} cm^{-2} and galvanostatic time-series), five cyclic voltammetry cycles from 0.05 to 1.00 V served as pretreatment.

Results

Figure 1 shows cyclic voltammograms (CV) in the absence of EG for the three distinct MOH electrolytes (M = Li, Na, and K). In this potential window, it is possible to recognize four regions as follows: Pt-H (I), the double layer region (II), Pt-OH (III), and Pt-O (IV). These profiles fully agree with the literature [32, 33] and the absence of sharp peaks in region I indicates the presence of well-prepared {111} terraces. Interestingly, the cation does not change the regions I, II, and the onset of OH^- adsorption but, once adsorbed, OH_{ad} is stabilized by hydrated cations in the sequence $Li^+ > Na^+ > K^+$ (Figure S1 in supplementary files brings all the CVs together). These noncovalent interactions between the hydrated cation

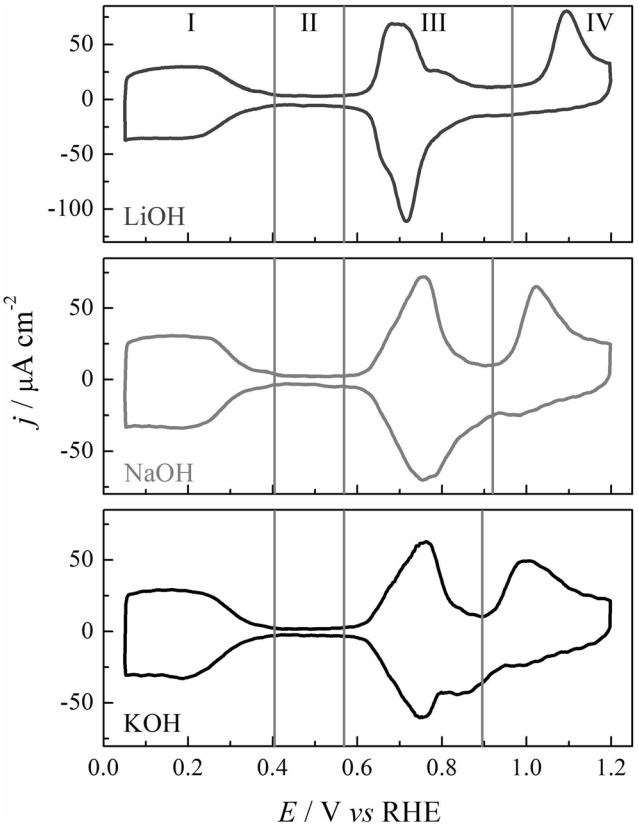

Fig. 1 Cyclic voltammograms of Pt(111) in 0.1 M MOH (M = Li, Na, or K) at 25 °C. $v = 0.050$ V s^{-1}

and adsorbed species shift the processes in regions III and IV to lower and higher potentials [29], respectively. The CVs are stable along the cycles since the potential does not exceed 1.20 V.

In acid media (0.1 M $HClO_4$), the transition from region III to IV is mediated by a plateau described as a kinetic barrier of stable water/OH_{ad} layer, forming an additional OH adsorption before the PtO growth [34]. Theoretical studies also claim that this kinetic barrier is due to the direct transition of 0.33 ML of OH_{ads} to 0.25 ML of O_{ads} [35], and recently, the presence of atomic oxygen was contested based on spectroscopy data, suggesting a (su) peroxide species instead [36]. Regardless of the transition mechanism, regions III and IV are composed of distinct species and, through similarities in CV shape, we extended these conclusions to the surface in alkaline media.

At low potential and in the presence of EG (0.05 M), regions I and II compete with alcohol adsorption producing surface poisoning species [37]. The oxygenated species in region III has been addressed to the increase of EGEO in Pt(111) and alkaline media which results in higher current densities than Pt(110), Pt(100) [38], or stepped Pt surfaces [39]. Although the oxidation current onset happens at considerably high potentials when compared with the others Pt(*hkl*), the nature of adsorbates or the stability of OH_{ad} layer allows the higher activity in Pt(111). Figure S2 shows that regardless

of the cation, the EGEO has the same onset potential at Pt(111); however, the current for potentials up to 1.0 V is lower when KOH is employed as supporting electrolyte. Sitta et al. [40] showed that at 0.8 V both current and EGEO products distribution depend on the electrolyte cation in Pt(poly) and alkaline media, i.e., both EG oxidation current and the activation of C–C bond (yielding carbonate instead of oxalate) follow the order $Li^+ < Na^+ < K^+$. The dependence between product distribution and electrolyte cation affects the fast dynamic during oscillatory EGEO [14], i.e., the oscillation pattern and frequency in each cycle; however, less influence is expected in the *drift* behavior in the time-series.

Figure 2a shows representative galvanostatic time-series collected in the presence of distinct cations at 10 °C. The current chosen for each experiment corresponds to the minimum current necessary to observe oscillations in galvanodynamic experiments at 44.4 μA s^{-1} cm^{-2} based on the normalization procedure described in ref. [41] (Figure S3 in supplementary files). In KOH solutions, the potential monotonically increases reaching E > 1.00 V after 80 s of polarization. We named this time as time-series length. Although the similar time is demanded to reach this potential in NaOH (100 s), potential oscillations are observed just before the potential jump to E > 1.20 V. Finally, replacing Na^+ by Li^+, the time-series length increases to 480 s and the potential oscillations are also more evident. The lower mean potential observed in time-series in the presence of Li^+ agrees with higher OH_{ad} coverage at lower potentials provided by this cation when compared with Na^+ and K^+ [42]. Figure 2 also presents two sliced parts of the time-series focusing on the onset of oscillations during EGEO reaction in both LiOH and NaOH solutions. Period 1, small amplitude oscillations centered in 0.84 V with mean oscillation frequency (*w*) of ca 8 Hz are observed during the first seconds of oscillatory behavior of EGEO in NaOH; however, over time, the amplitude increases and the oscillation frequency decreases, reaching 6 Hz in the last seconds before the potential jump to E > 1.20 V. This *drift* has origin in the coupling between the fast and, long-term, slow dynamic processes, i.e., while the oscillations occur, another set of processes are slowly changing some system conditions, resulting in progressive changes in oscillation features. When Na^+ is replaced by Li^+, oscillations at lower mean potential (0.81 V), lower initial frequency (ca 6 Hz) that hardly changes over time, and the evolution to more complex patterns such as period 2 are observed. This pattern is shown in the supplementary file section as Figure S4.

The time-series behavior in Fig. 2 is comparable with the EGEO reaction performed in Pt(poly) [14–16] in terms of both frequency and the applied current density. The differences emerge when the reaction occurs in KOH solution, since in Pt(poly), this electrolyte allows both high frequency and several oscillation patterns [16], but the oscillatory behavior is suppressed in Pt(111). Other differences are revealed analyzing the time-series from 5 to 20 °C temperature range as

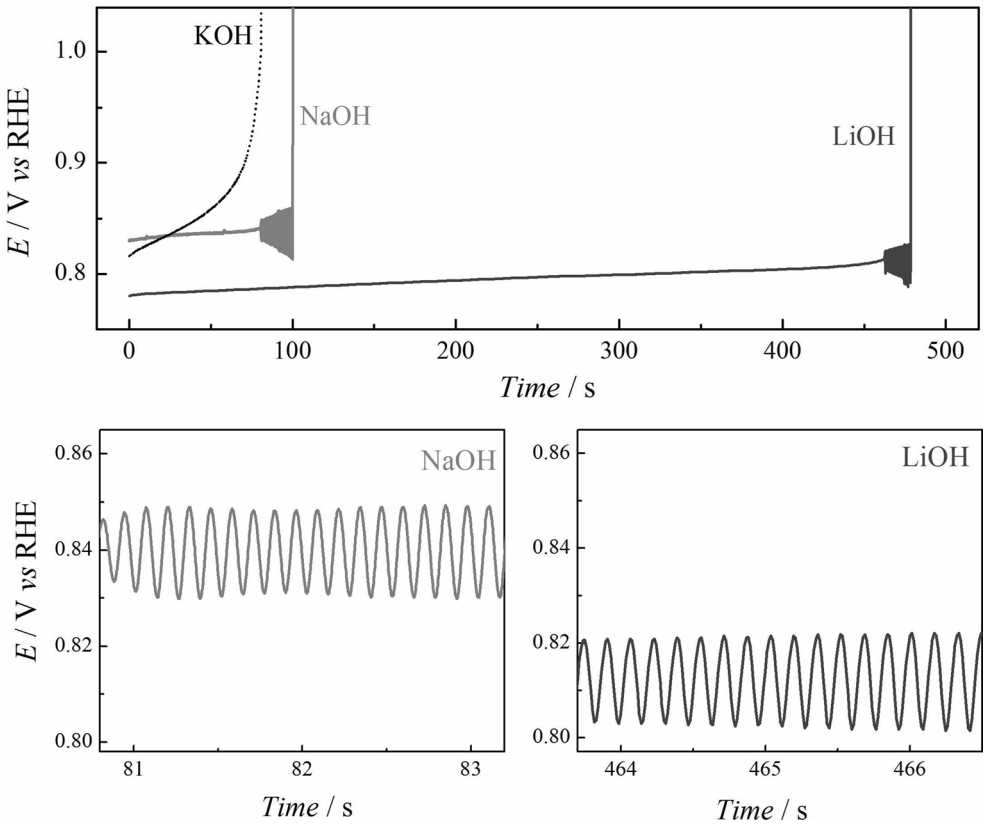

Fig. 2 Galvanostatic time-series EG electro-oxidation reaction in Pt(111) at 10 °C in the presence of 0.1 M LiOH ($j = 4.0$ mAcm^{-2}), NaOH ($j = 3.8$ mAcm^{-2}), or KOH ($j = 4.0$ mAcm^{-2}). The insets represent the onset of oscillations in the presence of Li^+ and Na^+, respectively

discussed in the sequence. In this work, we choose three experimental variables: time-series length, period 1 oscillation frequency, and maximum potential in oscillation cycles to follow the *drift* in time-series showing the important role of OH_{ad} and its conversion to O_{ad} in long-term EGEO dynamics.

The dependence of the time-series length on the electrolyte cation observed at 10 °C is kept in 5 to 15 °C temperature range (Fig. 3). While the time-series in Na^+ or K^+ electrolytes have similar lengths, the presence of Li^+ increases the series significantly. When the temperature is set at 20 °C, the time-series length becomes similar in LiOH and KOH electrolytes (this effect is discussed below). The time-series length can be related with the *drift*, since at fixed current, the potential increase over time represents the overpotential necessary to compensate the changes on the surface [21]. As mentioned above, irreversible oxide formation is the main cause of these changes, leading to the potential jump to high values. Thus, the stabilization of Pt(111)-OH provided by Li^+ slows down the formation of these oxides, increasing the time-series length. This cation effect on oxide formation has been also described for Au(111) surfaces [43].

The oscillation frequency, *w*, for a given period, is one of the most important parameters to be analyzed in a time-series, and it is defined as the inverse of the time demanded to reach two maximums or two minimums in a cycle. Period 1 oscillations during EGEO reaction in Pt in alkaline media show one of the highest *w* reported for small organic molecules [44]. Herein, the dependence of *w* with the temperature was employed to estimate the temperature coefficients (q_{10}) for each temperature variation (T1 and T2) (Table 1) following the equation [16]:

$$q_{10} = \left(\frac{\omega_{T2}}{\omega_{T1}}\right)^2$$

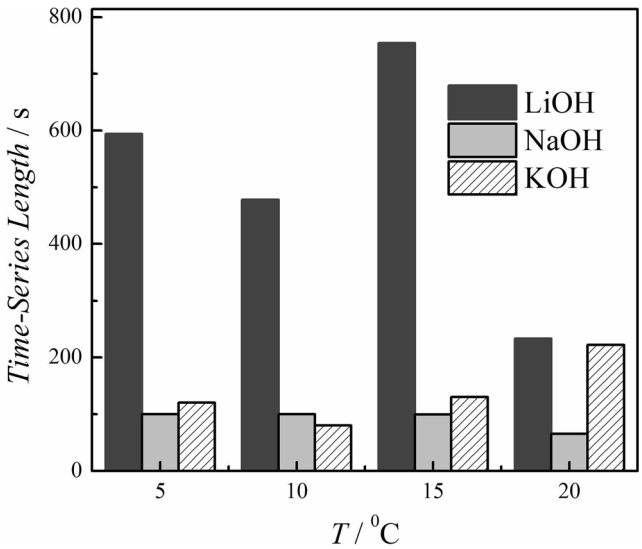

Fig. 3 Time-series length collected during EG electro-oxidation in Pt(111) in distinct temperatures and support electrolytes

Table 1 Temperature coefficients (q_{10}) based on mean oscillation frequency for EG electro-oxidation in Pt(111) and 0.1 M MOH (M = Li or Na)

	q_{LiOH}	q_{NaOH}
$\Delta T/^0C$		
5–10	1.1	1.3
10–15	3.4	1.0
15–20	1.5	1.1

q_{10} describes how sensitive a system is to temperature changes and the near 1 values obtained in most cases indicate the systems are in the so-called temperature compensation regime [16, 41], with small dependence on temperature (Figure S5 in supplementary files presents the onset of oscillatory behavior in time-series at distinct temperatures). This behavior agrees with previous data obtained in Pt(poly) [15, 16] and for the sake of the comparison under CV conditions in Pt(poly), q_{10} values are around two [16].

Although *w* hardly changes with temperature, there is a decrease in its value along the time-series. *w* was estimated in each cycle and a linear plot of log(*w*/Hz) versus time was obtained allowing to extract a slope (dlog(*w*)/dt) that was used to compare the *drift* in distinct temperatures and cations. Figure 4a presents an example of dlog(*w*)/dt for time-series shown in Fig. 2. Using this procedure, dlog(*w*)/dt was also estimated for the time-series in all studied temperatures. Figure 4b shows cation-dependent *w* evolutions, in which the presence of Li^+ decreases the changes when compared with Na^+ in the 5 to 15 °C temperature range. Since in KOH solution, the EGEO oscillations were inhibited; it was not possible to follow *w* in this system.

Finally, the maximum potential in each cycle is also an important descriptor for the time-series. The potential, as mentioned above, provides information about the nature of the surface species (OH_{ad} or oxides). During the EGEO reaction in LiOH solutions, the mean potential is lower than that in NaOH, as presented in Fig. 2a and discussed in terms of OH_{ad} layer; however, it is important to understand the potential changes during the oscillations. Thus, the maximum potentials (E_{max}) reached in each oscillation cycle were plotted against the time as shown in Fig. 4c and the slopes extracted from these curves are shown in Fig. 4d. Not surprisingly, the E_{max} evolution in NaOH is higher than in LiOH solutions from 5 to 15 °C.

The three parameters (time-series length, *w* and E_{max}) are related to Pt (hydro)oxides. Stabilizing the OH_{ad} and avoiding its conversion to oxides result in a decrease of the *drift* and this reflects on the increase of time-series length. Oscillation frequencies tend to decrease with the time (negative values in Fig. 4b) and this can be interpreted as a surface modification caused by oxide formation affecting the system's fast dynamic (oscillations). Finally, oxide formation seems to be less active for EGEO, as observed as a current decrease in high potential

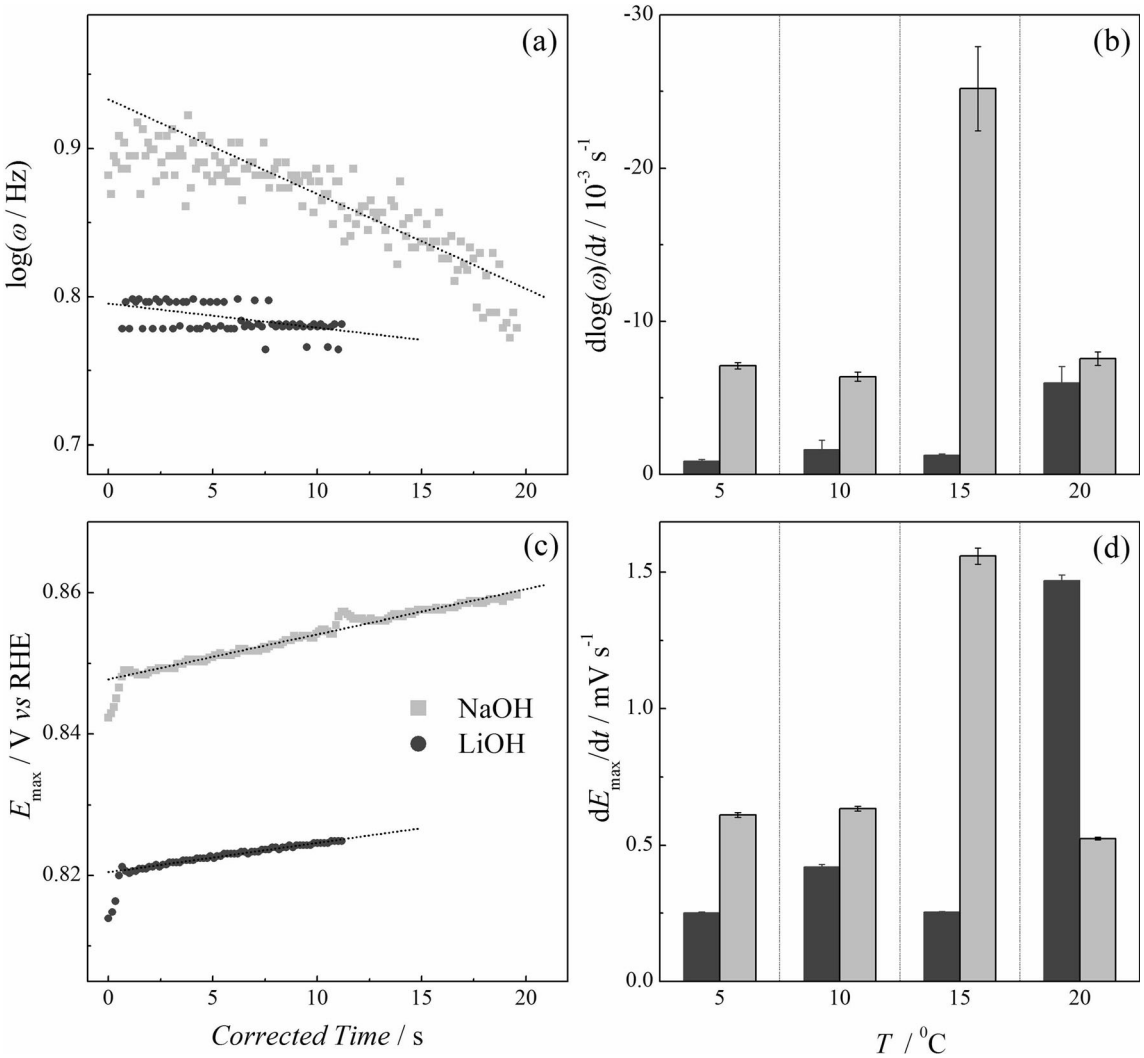

Fig. 4 Evolution of oscillation frequency (a) and maximum potential visited in each period one oscillation cycle (c) for EG electro-oxidation reaction at 10 °C. The slope of linear fits, represented as dotted lines, for ω and E_{max} are displayed in (b) and (d), respectively including the data for the time-series at 5, 10, 15, and 20 °C

CV profiles [38]; thus, the slow oxide formation during the transition from the region III to IV (Fig. 1) will trigger a potential increase in order to compensate the surface deactivation. However, the potential increase induces the oxide layer formation in a feedback loop. As a result, the Li^+ ability to stabilize the OH_{ad} layer, shifting the oxide formation and EGEO reaction to higher and lower potentials, respectively, is essential to maintain the oscillatory behavior in Pt(111). Apparently, this straightforward relation could not be applied to other Pt(*hkl*) or even polycrystalline surfaces, since the PtOH and PtO isotherms can coexist [27].

When the temperature exceeds 15 °C, some changes are observed in the above described tendencies. According to Markovic et al. [45], the temperature increase shifts the oxide formation to lower potentials, but the cation effect is unknown in this process and the OH_{ad} stabilization could be insufficient to compensate the increase of PtO nucleation and growth induced by the temperature. Moreover, non-monotonical behaviors were already described for formic acid electro-oxidation reaction in Pt(poly) in a 5 to 45 °C range [22], and explained based on distinct temperature dependence on irreversible oxide formation and surface poisons from the organic electro-oxidation reaction—EGEO in the present case. The non-monotonical changes at T < 25 °C described by the authors in ref. 22 for Pt(poly) are close to those observed in the present work. Thus, the changes observed in Fig. 3, especially the decrease of time-series length in LiOH electrolyte, could be related to increase of the transition from PtOH to PtO induced by the temperature. The effect is less pronounced in the other electrolytes once this transition is already fast at low temperatures.

Conclusions

In summary, the ethylene glycol electro-oxidation reaction was studied in Pt(111) in alkaline media focusing on the effect

of surface oxygenated species on oscillation dynamics. By means of OH_{ad} stabilization by noncovalent interaction with hydrated cations, the increase in time-series length accompanied by the decrease of both frequency and maximum potential (E_{max}) changes along the oscillations was observed These results contribute to understand the *drift* effect on oscillation time-series, providing experimental evidence that transition from OH_{ad} to oxides on Pt surfaces is an important parameter to be considered to describe and modeled time-series.

Acknowledgments The authors kindly thank Prof. JM Feliu for providing the single crystals employed in this work.

Funding information The São Paulo Research Foundation (FAPESP) (no. 2013/07296-2) has provided financial support and scholarship (no. 2016/14758-0) for this study. KNS received scholarship from the Brazilian Council for Scientific and Technological Development (CNPq) (no. 141097/2018-3).

References

1. Mukouyama Y, Kawasaki H, Hara D, Yamada Y, Nakanishi S (2017) Electrochem Soc 164(2):H1–H10
2. Mukouyama Y, Nakanishi S, Nakato Y (1999) Bull Chem Soc Jpn 72:2573–2590
3. Silva KN, Nagao R, Sitta E (2017) ChemistrySelect 2:11713–11716
4. Varela H, Krischer K (2002) J Phys Chem B 106:12258–12266
5. Strasser P, Lubke M, Raspel F, Eiswirth M, Ertl G (1997) J Chem Phys 107:979–990
6. Cabral MF, Nagao R, Sitta E, Varela H (2013) Phys Chem Chem Phys 15:1437–1442
7. Nagao R, Cantane DA, Lima FHB, Varela H (2012) Phys Chem Chem Phys 14:8294–8298
8. Nagao R, Cantane DA, Lima FHB, Varela H (2013) J Phys Chem C 117(29):15098–15105
9. Boscheto E, Batista BC, Lima RB, Varela H (2010) J Electroanal Chem 642:17–21
10. Martins AL, Batista BC, Sitta E, Varela H (2008) J Braz Chem Soc 19:679–687
11. Melle GB, Hartl FW, Varela H, Sitta E (2018) J Electroanal Chem 826:164–169
12. Silva KN, Maruyama ST, Sitta E (2017) J Braz Chem Soc 28(9): 1725–1731
13. Salum LF, Gonzalez ER, Feliu JM (2016) Electrochem Commun 72:83–86
14. Sitta E, Nagao R, Kiss IZ, Varela H (2015) J Phys Chem C 119(3): 1464–1472
15. Sitta E, Varela H (2010) Electrocatal 1:19–21
16. Sitta E, Nascimento MA, Varela H (2010) Phys Chem Chem Phys 12:15195–15206
17. Oliveira CP, Lussari NV, Sitta E, Varela H (2012) Electrochim Acta 85:674–679
18. Melle GB, Machado EG, Mascaro LH, Sitta E (2019) Electrochim Acta 296:972–979
19. Strasser P, Eiswirth M, Koper MTM (1999) J Electroanal Chem 478:50–66
20. Krischer K, Varela H (2003) In: Vielstich W, Lamm A, Gasteiger HA (eds) Handbook of fuel cells: fundamentals, technology and applications, vol. 2. Chichester, Wiley
21. Nagao R, Sitta E, Varela H (2010) J Phys Chem C 114:22262–22268
22. Zülke AA, Varela H (2016) Sci Rep 6:24553
23. Perini N, Batista BC, Angelo ACD, Epstein IR, Varela H (2014) ChemPhysChem 15:1753–1760
24. Melke AN, Nagao R, Eiswirth M, Varela H (2014) J Chem Phys 141:234701
25. Angestein-Kozlowska H, Conway BE, Sharp WBA (1973) J Electroanal Chem 43:9–36
26. Jerkiewicz G, Vatankhah G, Lessard J, Soriaga MP, Park YS (2004) Electrochim Acta 49:1451–1459
27. Wakisaka M, Suzuki H, Mitsui S, Uchida H, Watanabe M (2009) Langmuir 25:1897–1900
28. Aaronson BDB, Chen C-H, Li H, Koper MTM, Lai SCS, Unwin PR (2013) J Am Chem Soc 135:3873–3880
29. Strmcnik D, Kodama K, van der Vliet D, Greeley J, Stamenkovic VR, Markovic NM (2009) Nat Chem 1(6):466–472
30. Clavilier J, Armand D, Sun S, Petit M (1986) J Electroanal Chem 205:267–277
31. Korzeniewsky C, Climent V, Feliu JM (2012) In: Bard AJ, Zoski CG (eds) Electroanalytical chemistry: a series of advances, vol. 24. Boca Raton, CRC Press
32. Markovic NM, Ross PN (2002) Surf Sci Rep 45:117–229
33. Gomez-Marin AM, Rizo R, Feliu JM (2014) Catal Sci Technol 4: 1685–1698
34. Björling A, Feliu JM (2011) J Electroanal Chem 662:17–24
35. Bondarenko AS, Stephens IEL, Hansen HA, Pérez-Alonso FJ, Tripkovic V, Johansson TP, Rossmeisl J, Nørskov JK, Chorkendorff I (2011) Langmuir 27:2058–2066
36. Huang Y-F, Kooyman PJ, Koper MTM (2016) Nat Commun 7: 12440
37. Chang SC, Ho Y, Weaver MJ (1991) J Am Chem Soc 113:9506–9513
38. Markovic NM, Avramov-Ivic ML, Marinkovic NS, Adzic RR (1991) J Electroanal Chem 312:115–130
39. Sun S, Chen A (1994) Electrochim Acta 39:969–973
40. Sitta E, Batista BC, Varela H (2011) ChemComm 11:3775
41. Nagao R, Epstein IR, Gonzalez ER, Varela H (2008) J Phys Chem A 112:4617–4624
42. Stoffelsma C, Rodriguez P, Garcia G, Garcia-Araez N, Strmcnik D, Marković NM, Koper MTM (2010) J Am Chem Soc 132:16127–16133
43. Nakamura M, Nakajima Y, Kato K, Sakata O, Hoshi N (2015) J Phys Chem C 119:23586–23591
44. Machado EG, Varela H (2018) Kinetic instabilities in electrocatalysis In:Wandelt K (ed.) Encyclopedia of Interfacial Chemistry: Surface Science and Electrochemistry 5:701–718
45. Schmidt TJ, Ross PN, Markovic NM (2001) J Phys Chem B 105: 12082–12086